Automatic Disturbances Rejection Controller for Precise Motion Control of Permanent-Magnet Synchronous Motors

Y. X. Su, C. H. Zheng, and B. Y. Duan

***Abstract*—A highly robust automatic disturbances rejection controller (ADRC) is developed to implement high-precision motion control of permanent-magnet synchronous motors. The proposed ADRC consists of a tracking differentiator (TD) in the feedforward path, an extended state observer (ESO), and a nonlinear proportional derivative control in the feedback path. The TD solves the difficulties posed by low-order reference trajectories which are quantized at the sensor resolution, and the ESO provides the estimate of the unmeasured system's state and the real action of the unknown disturbances only based on a measurement output of the system. Simulations and experimental results show that the proposed ADRC achieves a better position response and is robust to parameter variation and load disturbance. Furthermore, the ADRC is designed directly in discrete time with a simple structure and fast computation, which make it widely applicable to all other types of derives.**

***Index Terms*—Disturbance rejection, friction compensation, nonlinear proportional derivative (NPD) control, observers, permanent-magnet synchronous (PMAC) motor.**

I. Introduction

With the rapid progress in power electronics, microprocessors, and control theory, permanent-magnet synchronous (PMAC) motors, which possess the characteristics of high power/weight ratio and inherent maintenance-free capability, have been recognized as one of the key components in automation and robots [1]–[9]. Conventionally, the linear control schemes dominate the controller market for PMAC motors [2]. However, the linear control design is based on a linear model and on the assumption that the mechanical and the electrical time constants differ at least for one order of magnitude. Apart from the fact that its formal treatment is inconsistent, linear control also does not allow a methodical design of the control structure and the determination of the optimal control parameters. The influence of nonlinearities, external disturbances (mechanical torque), and parameter and structural perturbations (inertia, friction) are usually considered only by the demanded "adequate robustness" of linear controllers. Consequently, the linear control cannot assure a satisfactory dynamic behavior in the entire operating range [2], [7]. Recently, many researchers have contributed their efforts toward high-precision control of PMAC motors, and various algorithms have been proposed [1]–[9].

In recent years, due to the great advances in nonlinear control theory, the observer-based controller has become one of the most commonly used schemes in industrial applications. The disturbances observers offer several attractive features. In the absence of large model errors, they allow independent tuning of disturbances rejection characteristics and command-following characteristics. Further, compared to integral action, disturbances observers allow more flexibility via the selection of the order, relative degree, and bandwidth of low-pass filtering [10]. Due to these attractive features, the observer-based controller has become one of the most commonly used schemes in control systems and an enormous amount of results on them have been published [9]–[17].

Furthermore, unmodeled nonlinear friction has been found to have an unwanted influence on control performance [2], [11], [18]–[21]. Usually, a model-based approach is employed to reduce the effect from friction [2], [18], [19]. Even in adaptive control of servo systems, an initial friction model is also crucial to ensure smooth control signals and rapid parameter convergence. However, in practical conditions, because of the inherent nonlinearity of friction, precise friction modeling has always been a difficult and challenging problem. Recently, extensive efforts have been made toward more advanced control of precision motion systems, based on a disturbances observer to implement the friction compensation [11], [20], [21].

In this paper, a discrete-time automatic disturbances rejection controller (ADRC) is designed to realize high precision motion control of PMAC motors. The nonlinear friction is considered as an unknown disturbance to the system, and an extended state observer (ESO) in the feedback path provides the estimate of the unmeasured state and the real action of the unknown nonlinear friction, only based on a position measurement. A tracking differentiator (TD) in the feedforward path solves the difficulties posed by low-order reference trajectories which are quantized at the sensor resolution, and a nonlinear proportional derivative (NPD) control is used to synthesize the control action. The effectiveness of this control scheme is verified by simulations and experimental results performed on a PMAC motor.

Manuscript received August 28, 2002; revised September 20, 2004. Abstract published on the Internet March 14, 2005. This work was supported by the National Natural Science Foundation of China under Grant 50075065, by the Robot Laboratory, Shenyang Institute of Automation, Chinese Academy of Science, under Grant RL200104, and by the Natural Science Foundation of Shaanxi Province under Grant 2000C22.

Y. X. Su and B. Y. Duan are with the School of Electro-Mechanical Engineering, Xidian University, Xi'an 710071, China (e-mail: yxsu@mail.xidian.edu.cn).

C. H. Zheng is with the School of Electronic Engineering, Xidian University, Xi'an 710071, China.

Digital Object Identifier 10.1109/TIE.2005.847583

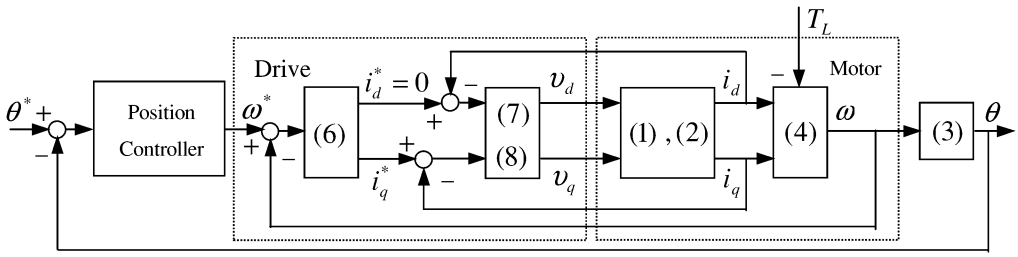

Fig. 1. Diagram of the motion control PMAC motor system.

The organization of this paper is as follows. A PMAC motor model is described in Section II. In Section III, the design of the ADRC is presented in detail, including the TD, ESO, and NPD with some simulations to verify their effectiveness. Simulations and experimental results on a PMAC motor are presented in Section IV. Finally, some concluding remarks are summarized in Section V.

II. Modeling of the PMAC Motor

The governing equation of a PMAC motor consists of two parts, electrical and mechanical. Taking the rotor coordinates (d–q axes) of the motor as reference coordinates, the linear model of a PMAC motor can be described as [2]

$$\frac{di_d}{dt} = -\frac{R}{L}i_d + N \cdot i_q \cdot \omega + \frac{1}{L}\upsilon_d \tag{1}$$

$$\frac{di_q}{dt} = -\frac{R}{L}i_q - \frac{KN}{L}\omega - N \cdot i_d \cdot \omega + \frac{1}{L}\upsilon_q \tag{2}$$

$$\frac{d\theta}{dt} = \omega \tag{3}$$

$$\frac{d\omega}{dt} = \frac{KN}{J}i_q - \frac{B}{J}\omega \tag{4}$$

where i_d and i_q are the currents on the d–q reference frame, respectively, and υ_d and υ_q are the voltages on the same frame, respectively, N is the number of pole pairs, R is the resistance of the stator, L is the inductance of the stator, K is the torque constant, ω is the angular velocity, B is the viscous friction coefficient, and J is the moment of inertia of the rotor.

A block diagram of the motion control of PMAC motor system is shown in Fig. 1, where the commonly used industrial ac servo drive is set in velocity mode. ω^* denotes the output of the position controller to the ac drive.

In the motor velocity mode for most ac servo drives used in industry, in general, the desired current component i_d^* in the d axis is set to zero. As a result, the desired perfect tracking error converges to zero in a manner such as [2]

$$\dot{e}_\omega + K_{P1} \cdot e_\omega + K_{I1} \cdot \int e_\omega dt = 0. \tag{5}$$

Then, the desired current component in the q coordinate i_q^* is

$$i_q^* = \frac{J}{KN}\left[\frac{T_L}{J} + \omega^* + K_{P1} \cdot e_\omega + K_{I1} \cdot \int e_\omega dt\right] \tag{6}$$

where ω^* is target velocity, $e_\omega = \omega^* - \omega$ is the tracking error, K_{P1} and K_{I1} are the proportional gain and integral gain of the velocity loop, respectively, and T_L is the external load.

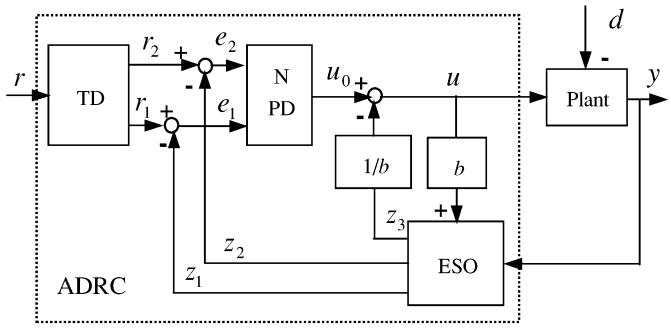

Fig. 2. Schematic diagram of ADRC.

To quickly reach the desired current component i_q^* in the q axis, the voltage control laws would be [2]

$$\upsilon_d = L\left[\frac{R}{L}i_d - N \cdot i_q \cdot \omega + \dot{i}_d^* - K_{P2} \cdot (i_d - i_d^*) - K_{I2} \cdot \int (i_d - i_d^*)dt\right] \tag{7}$$

$$\upsilon_q = L\left[\frac{R}{L}i_q + \frac{KN}{L}\omega + N \cdot i_d \cdot \omega + \dot{i}_q^* - K_{P2} \cdot (i_q - i_q^*) - K_{I2} \cdot \int (i_q - i_q^*)dt\right] \tag{8}$$

where K_{P2} and K_{I2} are the adjustable proportional and integral gains of the current loop, respectively, and $\dot{i}_d^*$ and $\dot{i}_q^*$ are derivatives of the currents i_d^* and i_q^*, respectively. Since $i_d^* = 0$, it is straightforward that $\dot{i}_d^* = 0$, and $\dot{i}_q^*$ can be obtained by differentiating (6) with respect to time.

III. ADRC Design

The schematic diagram of the ADRC is shown in Fig. 2, which consists of a TD in the feedforward path, an ESO, and an NPD synthesizer in the feedback path [22]. The TD in the feedforward path is motivated by the idea presented in [10], to solve the difficulties posed by low-order reference trajectories which are quantized at the sensor resolution. The ESO estimates the unmeasured state and the real action of the unknown disturbances to build a solid base for better performance and disturbances compensation. The NPD control is used to synthesize the control action. The design is carried on directly in discrete time and the structure chosen for realization permits fast computation and avoids the parameter sensitivity problem.

A. TD Design

In many practical situations, the performance of the controlled system is limited by how to select the high-quality differential signal from the noncontinuous noisy measured signal. In general, the differential signal is usually obtained by the backward difference (BD) of the given signal, which is very noisy and limits the overall performance [20]–[29]. To limit the amount of this noise, it is necessary to filter the differential signal. Additional delay is an unavoidable drawback of these conventional filters used frequently in industrial electronics [23]–[25]. This delay is particularly harmful when the filtered primary signal is to be used for time-critical feedback or synchronization purposes.

In this section, a TD [26] is used to provide a high-quality differential signal for more effective and robust performance in the presence of measurement noise. Although a rigorous stability analysis of TD has not been available, the viability for practical applications has been demonstrated via simulations and experiments [21], [22], [26]–[28].

For a boundary integrable function $r(t)$, system (9) can be used as a high-performance TD to provide two signals $r_1(t)$ and $r_2(t)$, such that $r_1(t) \to r(t)$ and $r_2(t) \to \dot{r}(t)$, respectively [26]–[28]

$$\begin{cases} r_1(k+1) = r_1(k) + hr_2(k) \\ r_2(k+1) = r_2(k) + h\text{fst}(r_1(k) - r(k), r_2(k), \delta_0, h_0) \end{cases} \tag{9}$$

where h is the sampling step, k denotes the kth sampling instant, h_0 a filtering factor which determines the suppression of noise, and δ_0 a velocity factor to determine the transition characteristics. The function $\text{fst}(x_1, x_2, \delta_0, h_0)$ is defined as

$$\text{fst}(x_1, x_2, \delta_0, h_0) = -\begin{cases} \delta_0 \text{sgn}(a), & |a| > d \\ \delta_0 \frac{a}{d}, & |a| \le d. \end{cases} \tag{10}$$

in which, $\text{sgn}(\cdot)$ denotes a standard sign function, and a and d can be determined as follows:

$$a = \begin{cases} x_2 + \frac{(a_0 - d)}{2}\text{sgn}(y), & |z| > d_0 \\ x_2 + \frac{z}{h_0}, & |z| \le d_0. \end{cases} \tag{11}$$

with

$$\begin{cases} d = \delta_0 h_0 \\ d_0 = h_0 d \\ z = x_1 + h_0 x_2 \\ a_0 = \sqrt{d^2 + 8\delta_0 |z|}. \end{cases} \tag{12}$$

It is noted that the developed TD has high robustness to the variation of the design parameters δ_0 and h_0. In general, large δ_0 is helpful to speed the transition and tracking, and large h_0 helps with the noise suppression. δ_0 can be chosen from the range of [5 10 000], and $h_0 = (2\text{–}25)h$. There is a tradeoff between the tracking and filtering.

The performance of the TD is shown in Fig. 3. The reference input is $r(t) = \sin(2t)$rad, $t = kh$, and it is perturbed by an additive white-noise component with the maximum amplitude of 0.01 rad. For comparison, the differential signal obtained by the general BD method is also plotted in this figure. The simulations were programmed in Matlab with a fourth-order Runge–Kutta and run on a PC Celeron-433. The simulation step was determined as $h = 0.005$, and all the initial values of r_1 and r_2 were set to zero. The design parameters for the TD were determined as follows: $h_0 = 5h$ and $\delta_0 = 6000$. It can be seen that the differential signal obtained by the developed TD is much better compared to that of the conventional BD method.

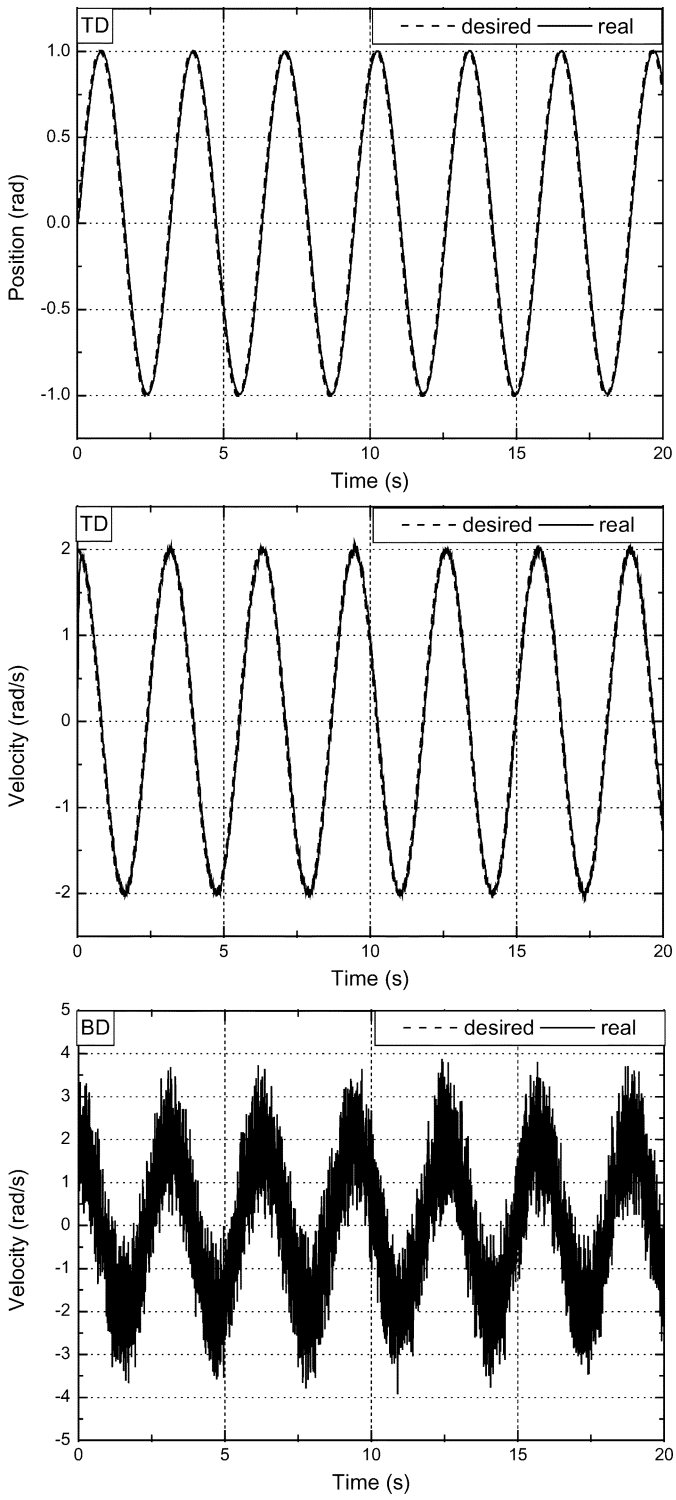

Fig. 3. Comparison of TD with general BD.

B. ESO Design

Consider a discrete uncertain nonlinear system with unknown disturbance

$$y^{(n)} = f\left(y, \dot{y}, \ldots, y^{(n-1)}, k\right) + d(k) + b_0 u(k) \tag{13}$$

where $f(y, \dot{y}, \ldots, y^{(n-1)}, k)$ is an unknown function, $d(k)$ is an unknown disturbance, $u(k)$ is the input to the system, and b_0 is a system parameter. Augmenting the variable $y^{(n)}$ into the state of the system, then the augmented state is the serial derivative of the measured state y. As a result, the $(n+1)$th-order ESO for this system based on the measured output $y(k)$ only can be constructed [28], [29], a shown by (14), at the bottom of the page, where $\alpha_i > 0 (i = 1, 2, \ldots, n), \beta_j > 0 (j = 1, 2, \ldots, n+1)$, and $\delta_1 > 0$ are design parameters. The nonlinear function $\text{fal}(x, \alpha, \delta)$ can be defined as

$$\text{fal}(x, \alpha, \delta) = \begin{cases} |x|^{\alpha}\text{sgn}(x), & |x| > \delta \\ \delta^{(\alpha-1)}x, & |x| \le \delta. \end{cases} \tag{15}$$

Note that, for this nonlinear ESO, it is an important fact that the extended state tracking the real action of the unknown disturbance, it is very helpful to realize the disturbance compensation. It is also noted that the developed ESO has high robustness to the variation of the design parameters. In general, $0 < \alpha_1 \le 1$ and $\alpha_i = \alpha_1 / 2^{i-1} (i = 2, \ldots, n), \delta_1$ can be chosen from the range of [0.0001 1], and small δ_1 is helpful for the noise suppression, $0 < \beta_j (j = 1, 2, \ldots, n+1)$ can be determined based on the tracking performance, and large β_j is helpful to speed the transition and the tracking. There is a tradeoff between δ_1 and β_j for a better noise suppression and tracking performance, from a noisy disturbed measurement.

To validate the effectiveness of the ESO, a simulation on a disturbed nonlinear system is carried out. The disturbed nonlinear system can be described as

$$\ddot{y} = -y^3 - y - 0.2\dot{y} + d \tag{16}$$

where d is an unknown disturbance, which can be expressed as $d = 0.5\text{sgn}(\cos(kh/2))$. For this second-order nonlinear system, the third-order ESO can be constructed as

$$\begin{cases} \varepsilon_0 = z_1(k) - y(k) \\ z_1(k+1) = z_1(k) + h(z_2(k) - \beta_1 \varepsilon_0) \\ z_2(k+1) = z_2(k) + h(z_3(k) - \beta_2 \text{fal}(\varepsilon_0, \alpha_1, \delta_1)) \\ z_3(k+1) = z_3(k) - h\beta_3 \text{fal}(\varepsilon_0, \alpha_2, \delta_1). \end{cases} \tag{17}$$

All the initial values of z_1, z_2, and z_3 were set to zero. For this third-order ESO, one feasible choice of the parameters was as follows: $\alpha_1 = 0.5, \alpha_2 = 0.25, \delta_1 = 0.000\,25, \beta_1 = 100, \beta_2 = 60, \beta_3 = 100$. The simulations were performed with and without the noise. The outputs z_1, z_2, and z_3 of the ESO and the outputs y_1 and y_2 of the system are shown in Figs. 4 and 5. It can be seen that the third-order ESO can estimate the system states and the real action of the unknown disturbance with high precision, even though in the presence of noise.

C. NPD Control and Disturbances Compensation

The linear proportional–integral–derivative (PID) controller is a widely used industrial controller which uses a linear combination of proportional, integral, and derivative action on the error to form the output of the controller. It is known that a linear combination of these components can achieve a compromised performance in terms of system response speed and stability. A nonlinear combination can provide an additional degree of freedom to achieve much improved system performance while still maintaining the advantages of simplicity and feasibility of linear PID control [30]–[33]. For this ADRC, an NPD control is used to synthesize the control action.

Once the high-quality differential signal has been obtained, the essential elements error e and its change c in classical PD control can be replaced by the following two components:

$$\begin{cases} e(k) = r_1(k) - z_1(k) \\ c(k) = r_2(k) - z_2(k). \end{cases} \tag{18}$$

Therefore, the primary control action of this ADRC can be synthesized [33]

$$u_0 = k_p \text{fal}(e, \alpha_3, \delta) + k_d \text{fal}(c, \alpha_4, \delta) \tag{19}$$

where k_p, k_d, α_3, α_4, and δ are design parameters.

With the feedforward control of the estimate of the real action of the unknown disturbances to cancel out their influences, the total control action of the proposed ADRC can be derived as

$$u = u_0 - \frac{z_3(k)}{b} \tag{20}$$

where b is a design parameter.

In fact, the above-described NPD control can be viewed as a magnitude-based gain-scheduling scheme. To further clarify this, we introduce the following equivalent gains, based on the

$$\begin{cases} \varepsilon_0 = z_1(k) - y(k) \\ z_1(k+1) = z_1(k) + h(z_2(k) - \beta_1 \varepsilon_0) \\ z_2(k+1) = z_2(k) + h(z_3(k) - \beta_2 \text{fal}(\varepsilon_0, \alpha_1, \delta_1)) \\ \vdots \\ z_n(k+1) = z_n(k) + h(z_{n+1}(k) - \beta_n \text{fal}(\varepsilon_0, \alpha_{n-1}, \delta_1) + b_0 u(k)) \\ z_{n+1}(k+1) = z_{n+1}(k) - h\beta_{n+1} \text{fal}(\varepsilon_0, \alpha_n, \delta_1) \end{cases} \tag{14}$$

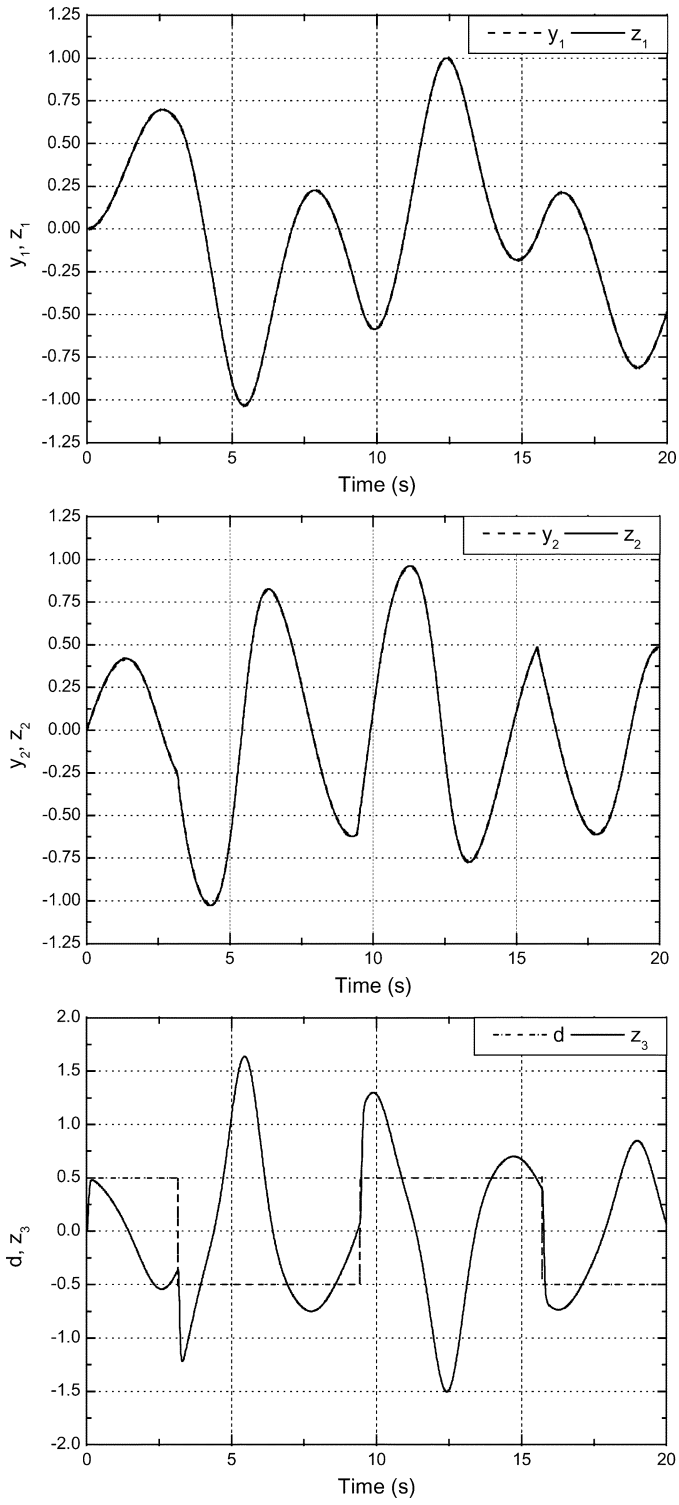

Fig. 4. Outputs of the third-order ESO and the system.

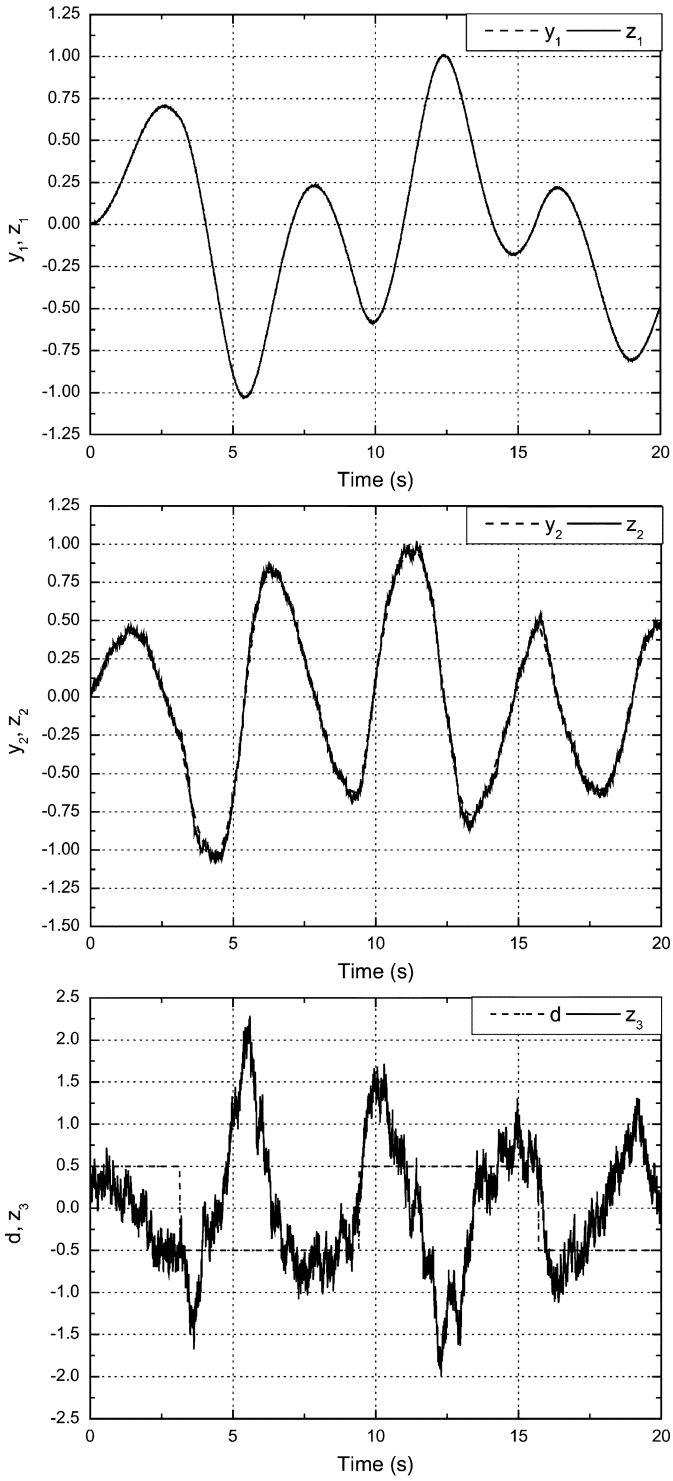

Fig. 5. Outputs of the third-order ESO and the system with noise.

property of $\lim_{x\to 0}(\mathrm{fal}(x,\alpha,\delta))/(x) = \delta^{\alpha-1}$ of the nonlinear function $\mathrm{fal}(x,\alpha,\delta)$:

$$\begin{cases} k_p^* = \beta_p \mathrm{fal}(e,\alpha_3,\delta)/e \\ k_d^* = \beta_d \mathrm{fal}(c,\alpha_4,\delta)/c. \end{cases} \tag{21}$$

It can be seen that the automatic gain adjustment is realized by the function $\mathrm{fal}(x,\alpha,\delta)$. First of all, we can determine the variation of the function $\mathrm{fal}(x,\alpha,\delta)$. A typical plot of the function $\mathrm{fal}(x,\alpha,\delta)$ with $\alpha = 0.25, 1.0$, and 1.5 while $\delta = 0.01$ is illustrated in Fig. 6. The equivalent gains k_p^* and k_d^* versus the state are shown in Fig. 7, with $k_p = 1.0, k_d = 1.0, \delta = 0.01, \alpha_3 = 1.5$, and $\alpha_4 = 0.75$. It can be seen that such variation of the gains results in rapid transit with elaborate damping. When the error is large, the enlarged proportional gain can generate a large correction to drive the system output to its goal rapidly. As the error diminishes, the reduced proportional gain and the enlarged derivative gain can generate an elaborate small correction to

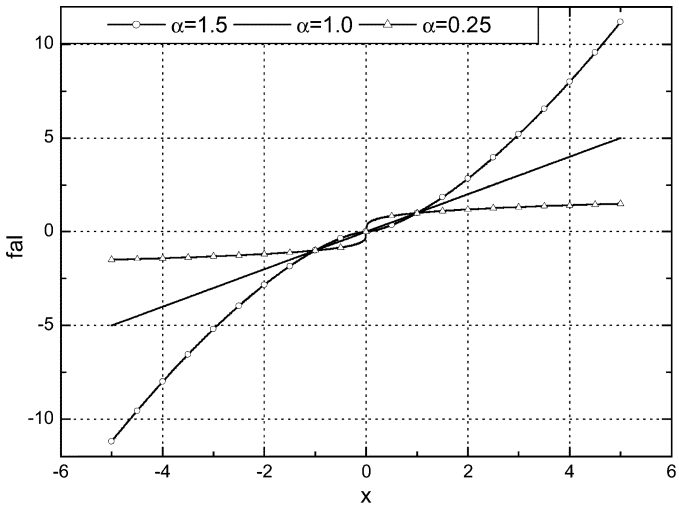

Fig. 6. $\mathrm{fal}(x, \alpha, \delta)$ function.

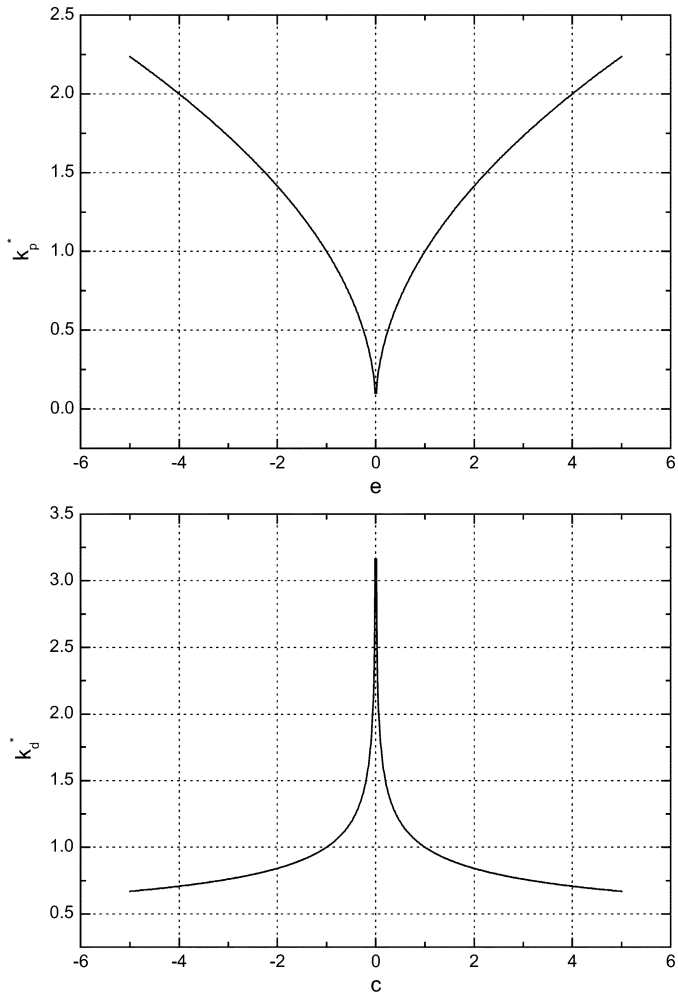

Fig. 7. Variation of the equivalent gains of the NPD control.

prevent excessive oscillations and large overshoots. Because of this automatic gain adjustment, the NPD control used exhibits the advantage of high initial proportional gain and low derivative gain to obtain a fast response, followed by a low proportional gain and large derivative gain to prevent oscillations. To achieve these gain characteristics, the parameters of the function

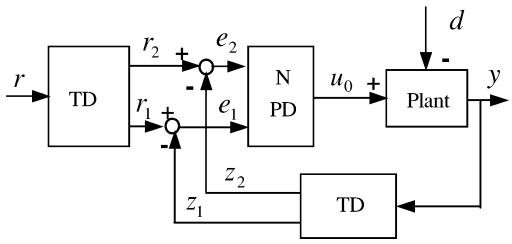

Fig. 8. Schematic diagram of NPD.

$\mathrm{fal}(x, \alpha, \delta)$ should be determined as: $\delta = 0.001$–0.1, $\alpha_3 > 1.0$, and $0 < \alpha_4 < 1.0$.

For a linear PD control system, it has been proven that there exists a suitable choice of the PD controller parameters so that the overall closed-loop system is globally asymptotically stable for position control [34]–[37]. Referring to the NPD control used, the proportional and derivative gains k_p and k_d can be determined by using the following guidelines to retain the stability of the closed-loop system: 1) the appropriate equivalent gains k_p^* and k_d^* of a standard linear PD control are determined first, by using many available tuning rules for linear PD control and 2i) the proportional and derivative gains k_p and k_d of the NPD control must be smaller than k_p^* and k_d^*, due to the increased gains of the above nonlinear transformation, which can be determined by the nonlinear function $\mathrm{fal}(x, \alpha, \delta)$.

IV. Simulations and Experimental Results

A. Simulations

The PMAC motor used in this research is an MSMA042A1G ac motor and the matched MSDA043A1A servo drive manufactured by Panasonic Inc. The specifications of the motor are: rated power, 0.4 kW; rated voltage, 200 V; rated current, 2.5 A; rated speed, 3000 r/min; $N = 4$, $R = 0.20\ \Omega$, $L = 0.0012$ H; $K = 0.18$ N·m/A; $J = 0.36 \times 10^{-4}$ kg·m^2; and $B = 8.56 \times 10^{-3}$ N·m·s/rad. An incremental optical encoder with a resolution of 4000 pulse/rev was used to provide the feedback position signal. The servo drive was set in the velocity mode, and the gains were selected as: $K_{P1} = 100$, $K_{I1} = 5$, $K_{P2} = 150$, and $K_{I2} = 80$, respectively.

The model equation given in (4) can be expanded in (22), under the assumption that the nonlinear friction is composed of the negative viscous friction and the Coulomb friction [11], [21]

$$J\frac{d\omega}{dt} = K \cdot N \cdot i_q - B \cdot \omega - f(\omega) \tag{22}$$

in which $f(\omega)$ can be expressed as [18], [21]

$$f(\omega) = \left(c_0 + c_1 e^{-c_2|\omega|}\right)\mathrm{sgn}(\omega) \tag{23}$$

where c_0, c_1 and c_2 are the characteristic parameters, which can be determined by the experiment.

In fact, the friction compensation proposed in this paper is not based on any friction model; it is only used for the simulation. Combining the practical operating condition and the results presented in [21], the friction characteristic parameters were selected as follows: $c_0 = 2.142$, $c_1 = 2.922$, and $c_2 = 86.956$. Besides the above-determined parameters for the TD and ESO

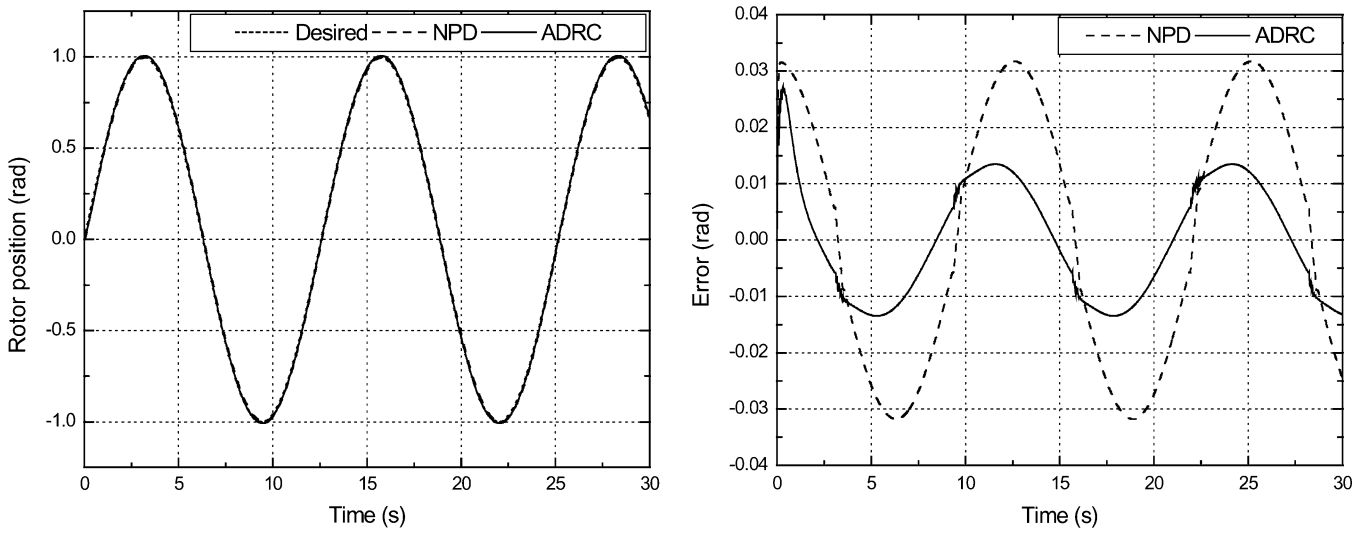

Fig. 9. Performance comparison between ADRC and NPD for $\theta^*(t) = \sin(0.5\,t)$ rad.

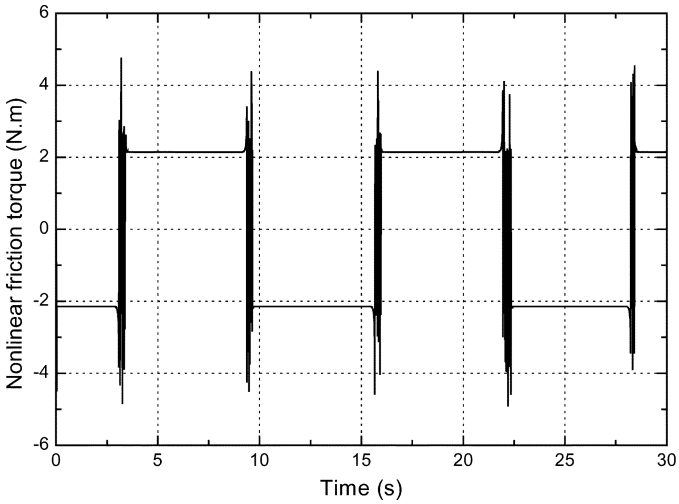

Fig. 10. Nonlinear friction torque for $\theta^*(t) = \sin(0.5\,t)$ rad.

in Section III, the other design parameters of the ADRC were determined as follows: $\delta = 0.01$, $\alpha_3 = 1.25$, $\alpha_4 = 0.5$, $k_p = 900$, $k_d = 3$, and $b = 1$.

For comparison, the NPD control expressed in (19) was also used for this motion control system. The schematic diagram of the NPD control is shown in Fig. 8. The proportional and derivative gains of the NPD control were determined as follows: $k_p = 1200$ and $k_d = 5$.

One way to access friction compensation is to measure the tracking error at relatively low speed, due to the fact that, at low speeds, a "stick–slip" phenomenon resulting from friction can lead to overshoot and large-amplitude limit cycles and will make the dominant contribution to the tracking error [2], [30]. Hence, the desired reference is a periodical sinusoidal profile of $\theta^*(t) = \sin(0.5t)$ rad. The simulation results are shown in Fig. 9 for the rotor position and tracking error. During the simulation, the nonlinear friction is shown in Fig. 10. It can be seen from these figures that the ADRC motion control PMAC motor system possesses better performance for friction compensation.

Fig. 11. Experimental setup.

B. Experimental Results

Fig. 11 shows the experimental setup, which consists of a six-channel D/A output card PCL-726 and a three-axes quadrature encoder card PCL-833. The control program was written in Borland C and run on an industrial computer made by Advantech Inc. The sampling period was determined as $T = 0.005$ s.

The following three experiments were carried out. The first experiment concerned the tracking performance of a periodical sinusoidal profile of $\theta^*(t) = \sin(0.5t)$ rad without load. The results with the ADRC and NPD are shown in Fig. 12. It can be seen that the ADRC achieves very good performance.

The second experiment concerned the performance robustness of the ADRC to parameter variation; a 6.0-kg payload was mounted on the motor shaft, so that the inertia load changed from $J = 0.36 \times 10^{-4}$ kg·m^2 to 5.05×10^{-4} kg·m^2. The experimental results with the ADRC and NPD to track $\theta^*(t) = \sin(0.5t)$ rad with this payload are shown in Fig. 13. Comparing Fig. 12 with Fig. 13, it shows that the ADRC achieves good tracking performance in spite of the change of inertia load.

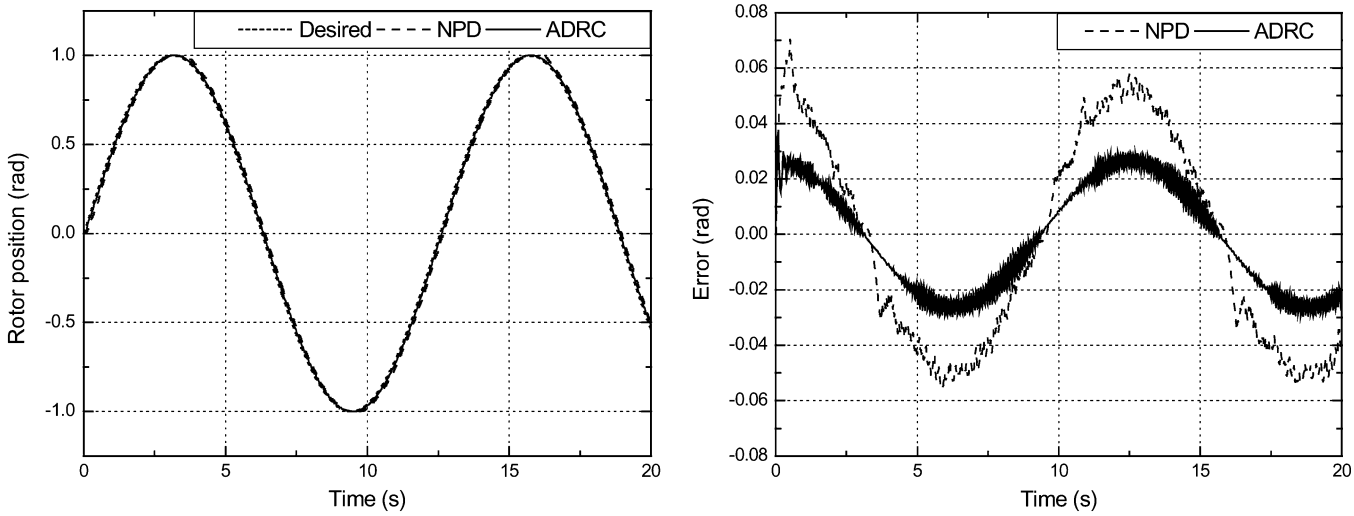

Fig. 12. Experimental comparison for $\theta^*(t) = \sin(0.5t)$ rad without load.

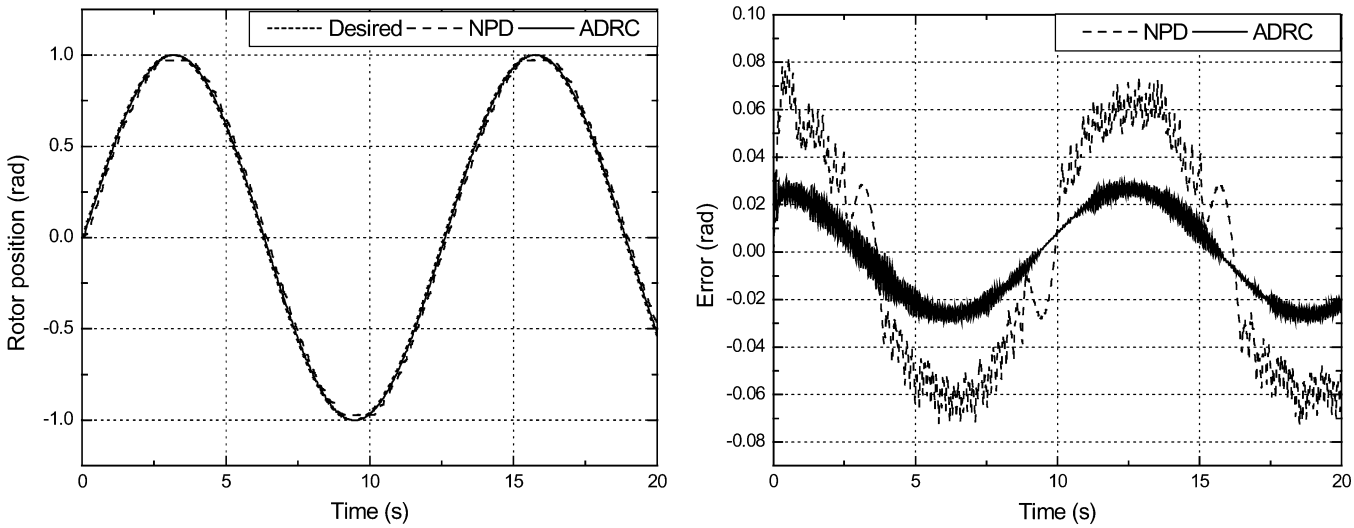

Fig. 13. Experimental comparison for $\theta^*(t) = \sin(0.5\,t)$ rad with load.

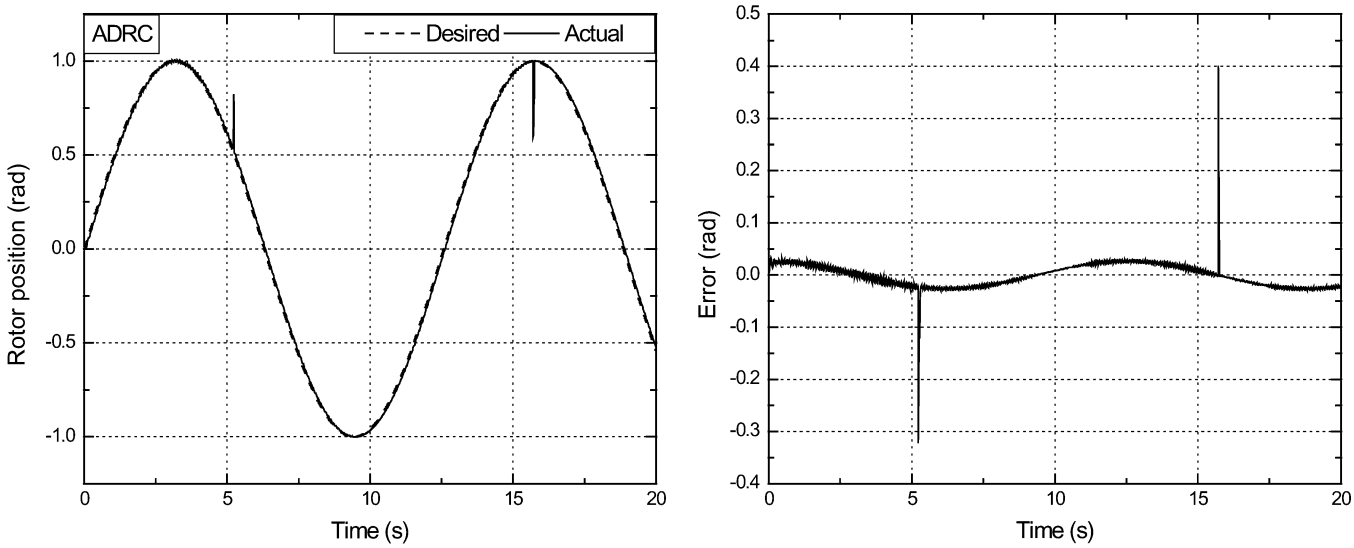

Fig. 14. Experimental result of ADRC with disturbance.

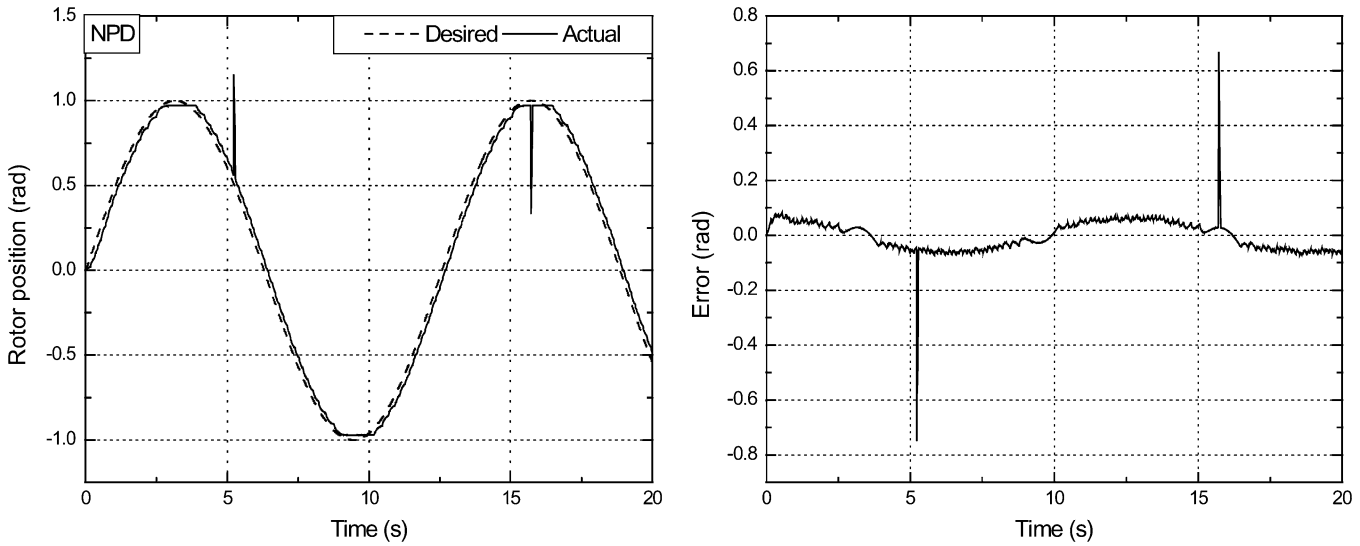

Fig. 15. Experimental result of NPD with disturbance.

The third experiment concerned the disturbance rejection of the proposed ADRC. A large step disturbance (a simulated position signal) described as follows is added:

$$d(t) = \begin{cases} 0, & \text{if } \cos(0.3t) > 0 \\ 0.5, & \text{if } \cos(0.3t) \le 0. \end{cases} \tag{24}$$

The results obtained by ADRC and NPD are shown in Figs. 14 and 15, respectively. Comparing Fig. 14 with Fig. 15, it can be seen that the added large disturbance does not affect the performance of the ADRC much, except for the spike when the sudden change of the disturbance occurs. This result illustrates the disturbance rejection of the ADRC.

From these experiments, it can be summarized that the ADRC possesses a much higher robustness against parameters variation and disturbances and, therefore, has better performance.

V. Conclusion

An ADRC has been developed for high-performance robust motion control of PMAC motors. The proposed ADRC is designed directly in discrete time with a simple structure and fast computation. The proposed controller uses a TD in the feedforward path to solve the difficulties posed by low-order reference trajectories which are quantized at the sensor resolution and an ESO in the feedback path to estimate the unmeasured state and the real action of the unknown disturbances, including nonlinear friction. The NPD control is used to synthesize the control action. The resulting controller achieves high precision in the presence of both parametric uncertainties and bounded disturbances, which provides a simple way to implement the nonlinear friction compensation without any model. Comparative simulations and experimental results demonstrate the high performance of the proposed ADRC strategy.

Acknowledgment

The authors would like to express their sincere gratitude to Prof. J. Q. Han at the Academy of Mathematics and System Sciences, Chinese Academy of Science, for his excellent guidance and detailed discussion regarding the determination of the parameters of the controller.

The authors are very thankful to the anonymous referees for the numerous remarks and suggestions which have lead to significant improvements of this paper.

References

[1] R. D. Lorenz, "Robotics and automation applications of drives and converters," *Proc. IEEE*, vol. 89, no. 6, pp. 951–962, Jun. 2001.

[2] G.-J. Wang, C.-T. Fong, and K. J. Chang, "Neural-network-based self-tuning PI controller for precise motion control of PMAC motors," *IEEE Trans. Ind. Electron.*, vol. 48, no. 2, pp. 408–415, Apr. 2001.

[3] R.-J. Wai, "Total sliding-mode controller for PM synchronous servo motor drive using recurrent fuzzy neural network," *IEEE Trans. Ind. Electron.*, vol. 48, no. 5, pp. 926–944, Oct. 2001.

[4] W. Leonhard, *Control of Electrical Drives*. Berlin, Germany: Springer-Verlag, 1996.

[5] F. J. Lin, R. F. Fung, and Y. C. Wang, "Sliding mode and fuzzy control of toggle mechanism using PM synchronous servomotor drive," in *Proc. IEE—Contr. Theory Appl.*, vol. 144, Sep. 1997, pp. 393–402.

[6] I.-C. Baik, K.-H. Kim, and M.-J. Youn, "Robust nonlinear speed control of PM synchronous motor using boundary layer integral sliding mode control technique," *IEEE Trans. Contr. Syst. Technol.*, vol. 8, no. 1, pp. 47–54, Jan. 2000.

[7] B. Grcar, P. Cafuta, M. Znidaric, and F. Gausch, "Nonlinear control of synchronous servo drive," *IEEE Trans. Contr. Syst. Technol.*, vol. 4, no. 2, pp. 177–184, Mar. 1996.

[8] D. G. Taylor, "Nonlinear control of electric machines: An overview," *IEEE Contr. Syst. Mag.*, vol. 14, no. 6, pp. 41–51, Dec. 1994.

[9] K.-K. Shyu, C.-K. Lai, Y.-W. Tsai, and D.-I. Yang, "A newly robust controller design for the position control of permanent-magnet synchronous motor," *IEEE Trans. Ind. Electron.*, vol. 49, no. 3, pp. 558–565, Jun. 2002.

[10] C. J. Kempf and S. Kobayashi, "Disturbance observer and feedforward design for a high-speed direct-drive positioning table," *IEEE Trans. Contr. Syst. Technol.*, vol. 7, no. 5, pp. 513–526, Sep. 1999.

[11] M. Iwasaki, T. Shibata, and N. Matsui, "Disturbance-observer-based nonlinear friction compensation in table drive system," *IEEE/ASME Trans. Mechatron.*, vol. 4, no. 1, pp. 3–8, Mar. 1999.

[12] S. Komada, M. Ishida, K. Ohnishi, and T. Hori, "Disturbance observer-based motion control of direct drive motors," *IEEE Trans. Energy Convers.*, vol. 6, no. 3, pp. 553–559, Sep. 1991.

[13] K.-H. Kim and M.-J. Youn, "A nonlinear speed control for a PM synchronous motor using a simple disturbance estimation technique," *IEEE Trans. Ind. Electron.*, vol. 49, no. 3, pp. 524–535, Jun. 2002.

[14] G. Zhu, A. Kaddouri, L.-A. Dessaint, and O. Akhrif, "A nonlinear state observer for the sensorless control of a permanent-magnet AC machine," *IEEE Trans. Ind. Electron.*, vol. 48, no. 6, pp. 1098–1108, Dec. 2001.

[15] E. Schrijver and J. van Dijk, "Disturbance observers for rigid mechanical systems: Equivalence, stability, and design," *Trans. ASME, J. Dyn. Syst., Meas., Contr.*, vol. 124, no. 4, pp. 539–548, 2002.
[16] C.-S. Liu and H. Peng, "Disturbance observer based tracking control," *Trans. ASME, J. Dyn. Syst., Meas., Contr.*, vol. 122, no. 2, pp. 332–335, 2000.
[17] W.-H. Chen, D. J. Balance, P. J. Gawthrop, and J. O'Reilly, "A nonlinear disturbances observer for robotic manipulators," *IEEE Trans. Ind. Electron.*, vol. 47, no. 4, pp. 932–938, Aug. 2000.
[18] B. Armstrong-Helouvry, P. Dipont, and C. Canudas de Wit, "A survey of models, analysis, tools, and compensation methods for the control of machines with friction," *Automatica*, vol. 30, no. 6, pp. 1083–1138, 1994.
[19] R. H. A. Hensen, M. J. G. van de Molengraft, and M. Steinbuch, "Frequency domain identification of dynamic friction model parameters," *IEEE Trans. Contr. Syst. Technol.*, vol. 10, no. 2, pp. 191–196, Mar. 2002.
[20] L. Xu and B. Yao, "Output feedback adaptive robust precision motion control of linear motors," *Automatica*, vol. 37, no. 7, pp. 1029–1039, 2001.
[21] K. K. Tan, T. H. Lee, and H. X. Zhou, "Micro-position of linear-piezoelectric motors based on a learning nonlinear PID controller," *IEEE/ASME Trans. Mechatron.*, vol. 6, no. 4, pp. 428–436, Dec. 2001.
[22] J. Q. Han, "Auto-disturbance-rejection controller and its applications" (in Chinese), *Contr. Decision*, vol. 13, no. 1, pp. 19–23, 1998.
[23] F. Janabi-Sharifi, V. Hayward, and C.-S. J. Chen, "Discrete-time adaptive windowing for velocity estimation," *IEEE Trans. Contr. Syst. Technol.*, vol. 8, no. 6, pp. 1003–1009, Nov. 2000.
[24] A. Jaritz and M. W. Spong, "An experimental comparison of robust control algorithms on a direct drive manipulator," *IEEE Trans. Contr. Syst. Technol.*, vol. 4, no. 6, pp. 627–640, Nov. 1996.
[25] M. Bodson, J. Chiasson, and R. T. Novotnak, "Nonlinear speed observer for high-performance induction motor control," *IEEE Trans. Ind. Electron.*, vol. 42, no. 4, pp. 337–343, Aug. 1995.
[26] J. Q. Han and L. L. Yuan, "The discrete form of tracking-differentiator" (in Chinese), *J. Syst. Sci. Math. Sci.*, vol. 19, no. 3, pp. 268–273, 1999.
[27] Y. X. Su, B. Y. Duan, and Y. F. Zhang, "Auto disturbance rejection motion control for direct-drive motors," in *Proc. IEEE IECON'02*, Seville, Spain, 2002, pp. 2073–2078.
[28] Y. X. Su, B. Y. Duan, C. H. Zheng, Y. F. Zhang, G. D. Chen, and J. W. Mi, "Disturbance rejection high precision motion control of a Stewart platform," *IEEE Trans. Contr. Syst. Technol.*, vol. 12, no. 3, pp. 364–374, May 2004.
[29] J. Q. Han, "The "extended state observer" of a class of uncertain system" (in Chinese), *Contr. Decision*, vol. 10, no. 1, pp. 85–88, 1995.
[30] B. Armstrong, D. Neevel, and T. Kusik, "New results in NPID control: Tracking, integral control, friction compensation, and experimental results," *IEEE Trans. Contr. Syst. Technol.*, vol. 9, no. 2, pp. 399–406, Mar. 2001.
[31] V. Parra-Vega and S. Arimoto, "Nonlinear PID control with sliding modes for tracking of robot manipulators," in *Proc. IEEE Int. Conf. Control Applications*, 2001, pp. 351–356.
[32] H. Seraji, "A new class of nonlinear PID controllers with robotic applications," *J. Robot. Syst.*, vol. 15, no. 3, pp. 161–181, 1998.
[33] J. Q. Han, "Nonlinear PID controller" (in Chinese), *Acta Autom. Sin.*, vol. 20, no. 4, pp. 487–490, 1994.
[34] S. Arimoto, *Control Theory of Non-Linear Mechanical Systems: A Passivity-Based and Circuit-Theoretic Approach*. Oxford, U.K.: Clarendon, 1996.
[35] P. Tomei, "Adaptive PD controller for robot manipulators," *IEEE Trans. Robot. Autom.*, vol. 7, no. 4, pp. 565–570, Aug. 1991.
[36] R. Kelly, "Global positioning of robot manipulators via PD control plus a class of nonlinear integral actions," *IEEE Trans. Autom. Contr.*, vol. 43, no. 7, pp. 934–938, Jul. 1998.
[37] H. Yazarel, C. C. Cheah, and H. C. Liaw, "Adaptive SP-D control of robotic manipulator in presence of modeling error in gravity regressor matrix: Theory and experiment," *IEEE Trans. Robot. Autom.*, vol. 18, no. 3, pp. 373–379, Jun. 2002.

Y. X. Su was born in Liaoning, China, in 1969. He received the B.Sc. and M.Sc. degrees in mechanical engineering from Gansu University of Technology, Lanzhou, China, in 1992 and 1995, respectively, and the Ph.D. degree in mechatronics from Xidian University, Xi'an, China, in 2002.

He is a Professor in the School of Electro-Mechanical Engineering, Xidian University. He was a Research Fellow for two years at City University of Hong Kong, Hong Kong. His research interests include mechatronics, motion control, robotics, and design optimization.

Prof. Su was awarded a Research Fellowship from the Alexander von Humboldt Foundation, Germany, in 2004.

C. H. Zheng was born in Xi'an, China, in 1969. She received the B.Sc. degree in electrical engineering from Xidian University, Xi'an, China, in 1991, and the M.Sc. degree in automatic control and applications from Gansu University of Technology, Lanzhou, China, in 1996. She is currently working toward the Ph.D. degree in signal processing in the National Key Laboratory of Radar Signal Processing, Xidian University.

From June 1996 to January 2000, she was a Teaching Research Assistant at the Xi'an Petroleum Institute, Xi'an, China. From February 2000 to February 2003, she was a Lecturer in the School of Electronic Engineering, Xidian University, where she is currently an Associate Professor. Her research interests include automation, fuzzy signal processing, and support vector machines.

B. Y. Duan was born in Hebei, China, in 1955. He received the B.Sc. and M.Sc. degrees from Northwest Telecommunication Engineering Institute, Xi'an, China, in 1981 and 1984, respectively, and the Ph.D. degree from Xidian University, Xi'an, China, in 1989.

From 1991 to 1994, he was a Postdoctoral Fellow at the University of Liverpool, Liverpool, U.K. He was also a Research Fellow at Hokkaido University, Hokkaido, Japan, from 1993 to 1994. He has also made brief academic visits to France and Australia. He is currently a Professor of Mechanical Engineering at Xidian University. He also serves as President of the university. His research has concentrated on structural optimization, CAD, and mechatronics.

Prof. Duan is a Member of the International Society of Computational Mechanics, a Fellow of the Chinese Institute of Electronics, Vice Chairman of the Society of Electromechanical Engineering in China, a Member of the Directing Committee of Mechanical and Electronic Engineering in China, a Member of the Expert Group of CAD Applied Engineering of Shaanxi Province, and Chairman of the Society of Electromechanical Engineering of Shaanxi Province.